Search for Invisible Decays of a Dark Photon Produced in e^+e^- Collisions at BABAR

selected highlights

outline

highlights of this paper

- physics picture of searching dark photon decays
  - to invisible dark matter particles
  - to visible ordinary standard model particles
- dedicated trigger lines for the low multiplicity single photon event
- BDT techniques has been used to further reduce background.

Physics picture of this work

- searches for dark matter interactions have so far yielded null results, it is postulated to interact very weakly with ordinary matter.
- The decay modes of dark photon depend on its mass and couplings, as well as the particle spectrum of the dark sector.
- In this paper, they assume the lowest-mass dark matter particle X is lighter than the half of the dark photon's mass.

Physics picture of this work

- under the assumption $m_\chi < m_{A'}/2$,
  the dominant decay mode is invisible, $A' \to \chi\bar{\chi}$

- The signal to be found in the detector is :

$$e^+e^- \to \gamma A'$$

search dark photon with lepton pairs

- if the previous assumption $m_\chi < m_{A'}/2$ not holds, then dominant dark photon decays are to visible SM particles
- There are lots of experiments performed such searching

[8] J. P. Lees *et al.* (*BABAR* Collaboration), Phys. Rev. Lett. **113**, 201801 (2014).
[9] D. Babusci *et al.* (KLOE-2 Collaboration), Phys. Lett. B **720**, 111 (2013); **736**, 459 (2014).
[10] J. R. Batley *et al.* (NA48/2 Collaboration), Phys. Lett. B **746**, 178 (2015).
[11] P. Adlarson *et al.* (WASA-at-COSY Collaboration), Phys. Lett. B **726**, 187 (2013).
[12] G. Agakishiev *et al.* (HADES Collaboration), Phys. Lett. B **731**, 265 (2014).
[13] H. Merkel *et al.* (A1 Collaboration), Phys. Rev. Lett. **112**, 221802 (2014).
[14] S. Abrahamyan *et al.* (APEX Collaboration), Phys. Rev. Lett. **107**, 191804 (2011).
[15] J. Blümlein and J. Brunner, Phys. Lett. B **731**, 320 (2014).
[16] S. Andreas, C. Niebuhr, and A. Ringwald, Phys. Rev. D **86**, 095019 (2012).

dedicated trigger lines

- To detect the low-multiplicity single-photon events, they designed dedicated trigger events.
- L1-hardware based level-1 trigger
  - select events at lease one EMC cluster with energy above 800 MeV.
- L3-software-based level-3 trigger
  - could reconstruct drift chamber tracks, EMC clusters, then select events.

BDT

- They try to further veto backgrounds by a multivariate boosted decision tree(BDT) discriminant, based on 12 discriminating variables.

- decision trees are powerful, but unstable.
  – small change in training data could produce large change in the tree.

BDT

- For boosting, the training events which were misclassified, that means a signal event fell on a background leaf or vice versa
  - their weights have been increased, which called boosted.
- then a new tree formed.
- this procedure repeated and many trees are built up.

BDT

selection of best tree

- the score from the m-th tree
  - +1 when the event falls on a signal leaf
  - -1 when the event falls on a background leaf
- final score is taken as a weighted sum of the scores of the individual leaves.

Questions from Tan Yuhang

R_L 和 R_T 的挑选范围的物理含义（是根据数据的什么量去挑选）？

这两者是不是也是于本底？值得大小有什么意义？

The event selection is optimized to minimize the expected upper limit on the $e^+e^- \to \gamma A'$ cross section $\sigma_{A'}$. Since the number of peaking $e^+e^- \to \gamma\gamma$ events cannot be reliably estimated and has to be determined from the fit to the data, this background limits the sensitivity to $e^+e^- \to \gamma A'$ at the low A' masses where the photon energies for the two types of events are indistinguishable. In this regime, we define a "tight" selection region $\mathcal{R}_T$ which maximizes the ratio ε_S/N_B for large N_B, and $\varepsilon_S/2.3$ in the limit $N_B \to 0$, where ε_S is the selection efficiency for the signal and N_B is the number of background events expected in the full data sample. We also require $-0.4 < \cos\theta^*_\gamma < 0.6$ in order to suppress $e^+e^- \to \gamma\gamma$ events in which one of the photons would have missed the central region of the EMC.

A "loose" selection region $\mathcal{R}_L$ maximizes $\varepsilon_S/\sqrt{N_B}$. This selection is appropriate at higher M_X where the background is well described by a featureless continuum distribution, and maximal $\varepsilon_S/\sqrt{N_B}$ corresponds to the lowest upper limit on the $e^+e^- \to \gamma A'$ cross section.

TABLE I. Data sets and event selections used in this Letter. The characteristic energies of each data set are listed in rows; the event selections described in the text in columns. The table entries list the integrated luminosity and the numbers of events selected by each data set.

Data set	LowM				HighM		
Data set	$\mathcal{L}$	Selection			$\mathcal{L}$	Selection	
		$\mathcal{R}_B$	$\mathcal{R}'_L$	$\mathcal{R}_T$		$\mathcal{R}_B$	$\mathcal{R}_L$
$\Upsilon(2S)$	15.9 fb^{-1}	22,590	42	6	15.9 fb^{-1}	405,441	324
$\Upsilon(3S)$	31.2 fb^{-1}	68,476	129	26	22.3 fb^{-1}	719,623	696
$\Upsilon(4S)$	5.9 fb^{-1}	7,893	16	9			

Question from Tan Yuhang

root of the Bayesian limit on ε^2 from Fig. 4. Our data rule out the dark-photon coupling as the explanation for the $(g-2)_\mu$ anomaly. Our limits place stringent constraints on

红线部分的结论是怎么从图 4 图 5 中得到的？本实验中的 limit 是指 A′ 质量的限制还是有更多的限制。

The 90% confidence level (C.L.) upper limits on ε^2 as a function of $m_{A'}$ are shown in Fig. 4. We compute both the Bayesian limits with a uniform prior for $\varepsilon^2 > 0$ and the frequentist profile-likelihood limits [29]. Figure 5 compares our results to other limits on ε in channels where A' is allowed to decay invisibly, as well as to the region of parameter space consistent with the $(g-2)_\mu$ anomaly [5]. At each value of $m_{A'}$ we compute a limit on ε as a square root of the Bayesian limit on ε^2 from Fig. 4. Our data rule out the dark-photon coupling as the explanation for the $(g-2)_\mu$ anomaly. Our limits place stringent constraints on

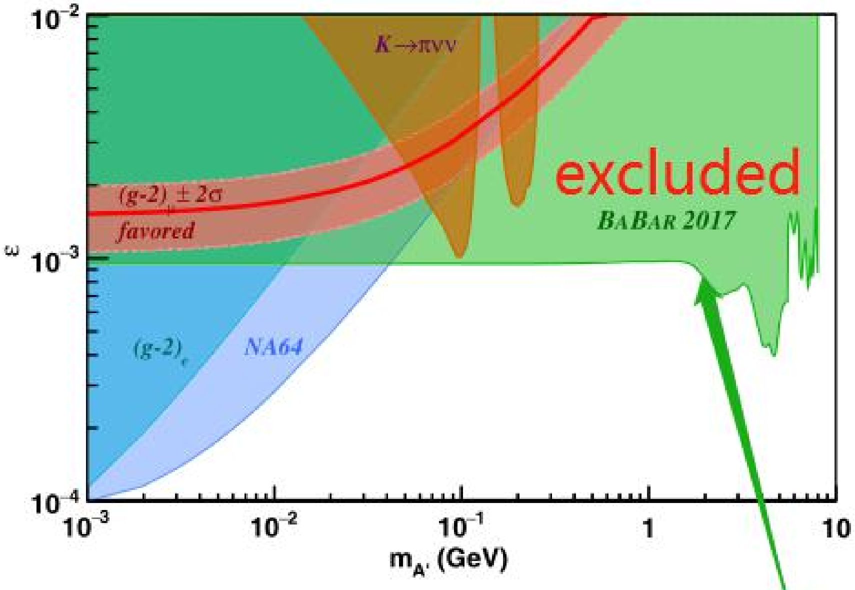

FIG. 5. Regions of the A' parameter space (ε vs $m_{A'}$) excluded by this work (green area) compared to the previous constraints [7,18–20] as well as the region preferred by the $(g-2)_\mu$ anomaly [5].